BNL-90506-2009-JA

QUANTIFYING RELATIONSHIP BETWEEN RELATIVE CLOUD RADIATIVE FORCING, CLOUD FRACTION AND CLOUD ALBEDO, AND THEIR MULTISCALE VARIATIONS

Liu, Y. and Wu, W.

Submitted to
Geophys. Res. Lett.

October 2009

Environmental Sciences Department/Atmospheric Sciences Division

Brookhaven National Laboratory
P.O. Box 5000
Upton, NY 11973-5000
www.bnl.gov

Notice: This manuscript has been authored by employees of Brookhaven Science Associates, LLC under Contract No. DE-AC02-98CH10886 with the U.S. Department of Energy. The publisher by accepting the manuscript for publication acknowledges that the United States Government retains a non-exclusive, paid-up, irrevocable, world-wide license to publish or reproduce the published form of this manuscript, or allow others to do so, for United States Government purposes.

This preprint is intended for publication in a journal or proceedings. Since changes may be made before publication, it may not be cited or reproduced without the author's permission.

DISCLAIMER

This report was prepared as an account of work sponsored by an agency of the United States Government. Neither the United States Government nor any agency thereof, nor any of their employees, nor any of their contractors, subcontractors, or their employees, makes any warranty, express or implied, or assumes any legal liability or responsibility for the accuracy, completeness, or any third party's use or the results of such use of any information, apparatus, product, or process disclosed, or represents that its use would not infringe privately owned rights. Reference herein to any specific commercial product, process, or service by trade name, trademark, manufacturer, or otherwise, does not necessarily constitute or imply its endorsement, recommendation, or favoring by the United States Government or any agency thereof or its contractors or subcontractors. The views and opinions of authors expressed herein do not necessarily state or reflect those of the United States Government or any agency thereof.

Quantifying Relationship between Relative Cloud Radiative Forcing, Cloud fraction and Cloud Albedo, and Their Multiscale Variations

Yangang Liu* and Wei Wu

(Brookhaven National Laboratory, Bldg. 815E, Upton, NY 11973, USA; lyg@bnl.gov)

Abstract

Cloud radiative forcing, cloud fraction, and cloud albedo have been widely used to study cloud effects on radiation budget; however, their mutual relationship and multiscale variations are not well quantified. Here a new analytical relationship between the three quantities is formulated. The analytical expression is further applied to derive, for the first time, a long-term, time series of cloud albedo by using concurrent surface-based measurements of downwelling surface shortwave radiation and cloud fraction collected by the US Department of Energy's Atmospheric Radiation Measurement (ARM) Program at the Great Southern Plains (SGP) site since 1997. The time series of relative shortwave radiative forcing, cloud fraction and cloud albedo are examined for their diurnal, annual and inter-annual variations. The results show that all three quantities exhibit strong diurnal and annual cycles but less interannual variability. The relative shortwave cloud forcing varies in phase with cloud fraction, and the 2-m relative humidity.

1. Introduction

Quantifying the impact of clouds on the Earth's radiation budget has been the subject of intensive research [Schneider, 1972; Charlock and Ramanathan, 1985; Ramanathan, 1987; Laszlo and Pinker, 1993; Ramanathan et al., 1989; Harrison et al. 1990; Arking, 1991, 1999; Kiehl, 1994; Wielicki, 1995; Rossow and Zhang, 1995; Raschke et al., 2005]. One of the quantities that have been widely used to gauge the radiative impact of clouds is cloud radiative forcing [CRF, e.g., Ellis, 1978; Coakley and Baldwin, 1984; Charlock and Ramanathan, 1985; Ramanathan, 1987; Cess 1987]. Advantages of using CRF are that it can be obtained directly from satellite observations at the top of atmosphere (TOA), and can be readily calculated by global climate models (GCMs). Comparison of model-simulated CRF against satellite observations have proven to be instrumental in evaluation of climate models and the identification of cloud feedbacks and parameterizations as the factors contributing most to the uncertainty in estimates of the model climate sensitivity (Cess et al., 1997, 2001; Potter and Cess, 2004). The other two commonly used cloud quantities are cloud fraction [Schnieder, 1972; Bony and Dufresne, 2005] and cloud albedo (Wielicki et al., 2005; Bender et al., 2006).

Despite the great efforts and advances over the past few decades, much remains unsolved. None of these three quantities is fully understood, nor are they well represented in GCMs. For example, Bender et al [2006] compared the results of global albedo from 22 GCMs and two satellites, and found that GCM-derived values not only exhibit a large spread but also consistently higher values than those observed by the two satellites. These differences between observations and models are likely due to inadequate GCM parameterizations of cloud albedo.

Representation of cloud fraction, especially for low-level clouds, suffers serious problems as well [Bony and Dufresne, 2005]. Still less understood are the quantitative relationship between CRF, cloud fraction and cloud albedo, and how these quantities vary over multiple scales. Particularly challenging are issues related to cloud albedo; our knowledge on it has relied mainly on limited aircraft in situ measurements, indirect satellite measurements, and theoretical investigation. No ground-based techniques are available that allow for long-term measurements.

To fill this gap, here we first present an analytical formulation of the relationship between the surface shortwave CRF, cloud fraction, and cloud albedo, and derive an analytical expression relating cloud albedo to the relative surface shortwave CRF and cloud fraction. This expression is then applied to obtain time series for cloud albedo from the decade-long surface-based measurements of downwelling SW radiation flux and cloud fraction collected by the U.S. Department of Energy's Atmospheric Radiation Measurement (ARM) program at the Southern Great Plain (SGP) site since 1997 (Stokes and Schwartz 1994; Ackerman and Stokes 2003). The decade-long datasets are then examined to determine their multiscale variabilities and underlying physics.

2. Analytical relationship between cloud radiative forcing, cloud fraction and cloud albedo

2.1. Concept of relative cloud-radiative forcing

Cloud radiative forcing (CRF) was originally proposed as the difference between clear-sky and all-sky net radiation fluxes, and was first applied to study radiation budgets measured with satellites at the top of atmosphere (TOA) [Ellis, 1978; Coakley 1984; and Charlock and Ramanathan, 1985; Ramanathan, 1987; Cess, 1987]. Indirect methods are often used to infer the

surface CRF from TOA radiation fluxes using some physical or regression model since no direct satellite measurement of surface radiation fluxes is possible (e.g., Laszlo and Pinker, 1993; Li et al, 1993). Surface CRF has been later studied using surface-based radiation measurements [Dong et al. 2002; Mace et al., 2006; Mace and Benson 2008]. Despite the usefulness and popularity, the CRF thus defined suffers from the drawback of being affected by factors other than clouds [e.g., solar zenith angle, definition of what constitutes a clear-sky reference, and specification of the surface albedo], and much effort has been devoted to minimizing the effects of these non-cloud factors on computation of the CRF [Li et al., 1995; Imre et al., 1996; Li and Trishchenko, 2001; Vavrus, 2006; Betts and Viterbo, 2005; Betts, 2007; Betts et al., 2009]. Among existing attempts, the non-dimensional measure proposed by Betts and his co-workers is probably the best, and is detailed below for the surface shortwave CRF.

The surface shortwave CRF (F_{cld}) is defined in terms of downwelling flux such that,

$$F_{cld} = F_{all}^{dn} - F_{clr}^{dn} \tag{1}$$

where F_{all}^{dn} and F_{clr}^{dn} denote the all-sky and clear-sky surface downwelling SW radiation fluxes, respectively, with positive values being indicative of downward fluxes. Replacing net flux with downwelling flux reduces the effect of surface albedo [see Vavrus, 2006 for more discussion]. To further minimize the effects from other non-cloud factors, Betts and Viterbo [2005] proposed a non-dimensional measure for the surface CRF defined as [see also Betts, 2007 and Betts et al. 2009],

$$\alpha_{cld}^{SRF} = -\frac{F_{cld}}{F_{clr}^{dn}} = 1 - \frac{F_{all}^{dn}}{F_{clr}^{dn}} \tag{2}$$

They named this new quantity α_{cld}^{SRF} as the surface effective cloud albedo. But, as will become evident later, "effective cloud albedo" is a misnomer because the variation of α_{cld}^{SRF} is associated more with cloud fraction than with cloud albedo, and is generally related to cloud absorptance as well. Accordingly, in this paper, α_{cld}^{SRF} is referred to as relative surface shortwave CRF.

2.2. Analytical formulation

Betts and his coworkers [Betts and Viterbo, 2005; Betts, 2007 and Betts et al. 2009] examined α_{cld}^{SRF} derived from the International Satellite Cloud Climatology Project (ISCCP) data over several river basins in comparison with those from different the reanalysis data (ERA-40 and ERA-Interim). Although attempts have been made to connect α_{cld}^{SRF} to cloud fraction and cloud albedo, quantitative relationship between the three quantities still remains elusive, and is a focus of this section.

As a first-order approximation, we consider a homogeneous atmosphere comprising a portion of clear air and a single cloud layer with cloud fraction *f*, cloud albedo α_r , and cloud absorptance α_a . For this simplified atmosphere, the all-sky surface downwelling shortwave radiation flux is given by

$$F_{all}^{dn} = (1-\alpha_r)(1-\alpha_a) f F_{clr}^{dn} + (1-f) F_{clr}^{dn} \tag{3}$$

Substitution of (3) into (2) yields the following expression:

$$\alpha_{cld}^{SRF} = (\alpha_r + \alpha_a - \alpha_r \alpha_a) f \tag{4a}$$

Equation (4a) reveals that α_{cld}^{SRF} is an increasing function of *f*, α_r, and α_a, which becomes more evident by ignoring the second-order term, $\alpha_r \alpha_a$, i.e.,

$$\alpha_{cld}^{SRF} = (\alpha_r + \alpha_a) f \tag{4b}$$

Furthermore, because α_a is generally much smaller than α_r [e.g., Fig. 4 of Gautier and Landsfeld, 1997), neglect of shortwave absorption further simplifies (4b) to

$$\alpha_{cld}^{SRF} = \alpha_r f \tag{4c}$$

Equation (4c) reveals that α_{cld}^{SRF} is essentially a product of f and α_r, and $\alpha_{cld}^{SRF} = \alpha_r$ under the overcast sky when *f* =1. Empirical evidence for the latter prediction was documented in an earlier study (Shi, 1994). This study also introduced the concept of relative surface CRF as defined by (2), but it was only concerned with overcast scenarios. Equation (4c) further reveals that the uncertainty in reported values of CRF simulated by different GCMs arises likely from inadequate treatments of both α_r and *f*.

2.3. New approach for measuring cloud albedo

At present, long-term records of cloud albedo have been primarily relied on satellite and earthshine measurements. But, the two techniques essentially measure global albedo, which depends on cloud albedo, cloud fraction and surface reflective properties. Furthermore, the estimates of global albedo obtained with these two techniques differ so much that even the sign of change in global albedo differs [Wielicki et al., 2005]. Obviously, the need for an approach that allows for long-term measurements of cloud albedo cannot be overemphasized. An

approach that utilizes surface-based remote sensing techniques as used at the ARM SGP site is even more desirable in view of the widely demonstrated fidelity of these remote sensors.

Equation (4c) suggests just such a technique if α_{cld}^{SRF} and *f* can be measured, i.e.,

$$\alpha_r = \frac{\alpha_{cld}^{SRF}}{f} \quad . \tag{5}$$

ARM has provided high-quality continuous measurements of multiple quantities essential to cloud-radiation interactions by integrating multiple surface-based remote sensors at the SGP site; especially useful to this study is the datastream with measurements of surface downwelling SW radiation fluxes and cloud fraction (www.arm.gov/data/sgp15swfanalsirs1longC1.c1). The original datastream has a 15-min resolution and covers the period of 25 March 1997 to 31 July 2009. Therefore, we can first obtain the series of α_{cld}^{SRF} from the surface radiation measurements using (2), and then substitute data on α_{cld}^{SRF} and *f* into (5) to obtain the data on cloud albedo.

3. Multiscale variations at the ARM SGP site

Systematic examination of α_{cld}^{SRF} only started very recently by Betts and his coworkers by using indirect satellite surface radiation measurements. No similar study has been reported using the direct surface-based, high-resolution ARM measurements at the SGP site. The 15-min data are further aggregated to examine the diurnal (Figure 1a), annual (Figure 1b) and interannual variations (Figure 1c) of α_{cld}^{SRF}, f, and α_r. A few points can be drawn from the figure. First, all three quantities exhibit strong diurnal and annual variations. Although the diurnal cycle is not complete due to missing nighttime downwelling shortwave radiation flux measurements, the

minima around local noon (GMT noon minus 6 hours) are remarkably obvious, with 0.26, 0.48 and 0.52 for α_{cld}^{SRF}, f and α_r, respectively. Two maxima appear for α_{cld}^{SRF} and *f*. The first occurs in local morning (0.41, 0.71 and 0.59 for α_{cld}^{SRF}, f and α_r) and the second in local afternoon (0.32, 0.59 and 0.60 for α_{cld}^{SRF}, f and α_r). On monthly scales, the summertime minima are evident, with α_{cld}^{SRF} = 0.19 and f = 0.41 in July any α_r = 0.45 in August. The maxima for α_{cld}^{eff} (0.30) and f (0.56) occur in March while for α_r (0.57) in October. The basic characteristics of the diurnal (morning maximum and noon minimum during daytime) and annual (wintertime maximum and summertime minimum) variations of cloud fraction are consistent with previous analyses [e.g., Lazarus et al., 2000; Dong et al. 2006; Kollias et al., 2007]. The annual variation of α_{cld}^{SRF} is similar to that observed in other continental areas such as Amazon and Missouri [Betts, 2007, 2009; Betts et al. 2009]. Second, these quantities exhibit much lower interannual than annual variations; the 13 yearly averages of α_{cld}^{SRF}, f and α_r are 0.26, 0.50 and 0.52, respectively.

The third point is especially noteworthy. Although the three quantities tend to vary largely in phase, the variation of α_{cld}^{SRF} is correlated more with *f* than α_r. This can be seen more clearly in Figure 2 (a, b). Together with (4), the higher correlation with *f* suggests that *f* varies slightly more than α_r. The in-phase relationship between α_{cld}^{SRF} and f was also found in Betts et al. [2009].

Figure 2 c and d further show α_{cld}^{SRF} as a function of the 2m air temperature and relative humidity to diagnose the underlying physics. The close correlation with the relative humidity

appears consistent the notion that the minimum occurrence of low-level clouds is often related to dryness and cloud thinning associated with high temperature [Del Genio and Wolf, 2000; Betts et al., 2009]. Also noteworthy is that α_{cld}^{SRF} , f and relative humidity are correlated to one another on all the temporal scales (diurnal, monthly and annual).,.

4. Concluding remarks

An analytical relationship between the relative surface shortwave cloud radiative forcing, cloud fraction and cloud albedo is derived. The analytical relationship not only reveals that the relative surface shortwave cloud radiative forcing is approximately a product of cloud fraction and cloud albedo, it also suggests a new approach to inferring cloud albedo from concurrent measurements of surface downwelling shortwave radiative fluxes and cloud fraction. This new technique is extremely valuable for surface-based sites such as the ARM SGP site where decade-long measurements of surface downwelling shortwave radiative fluxes and cloud fraction are available.

The decade-long high resolution data on the relative surface shortwave cloud radiative forcing, cloud fraction and cloud albedo are examined to discern their diurnal, annual and interannual variations. The results show that the variation of the relative surface shortwave cloud radiative forcing more closely follows variations in cloud fraction than cloud albedo, reinforcing the notion that the name “effective cloud albedo” originally suggested by Betts and his coauthors is inappropriate for representing normalized surface shortwave cloud radiative forcing. All three variables exhibit a noon minimum. The annual variations present a maximum

in wintertime and a minimum in summertime. No discernable trends exist in the interannual variations of all the three quantities.

It is noteworthy that the ideas presented here can be applied to the continuus data available from other ARM sites, and can be extended to TOA data, and to longwave radiation. Such extension likely provides additional information such as cloud shortwave absorptance and longwave emissivity. Another powerful application of this approach and data thus obtained is to validating cloud parameterizations by comparing the data derived from observations and corresponding GCM or other model simulations. Model evaluation against observations is essential to identifying model deficiencies [Betts et al., 2009].

Acknowledgment: This work is supported by the ASR (Atmospheric Science Research) and CCPP (Climate Change Prediction Program) programs of the U. S. Department of Energy. Dr. Peter H. Daum at the Brookhaven National Laboratory provides careful reading and valuable comments.

References

Ackerman T. P., and G. M. Stokes (2003), The Atmospheric Radiation Measurement Program, *Phys. Today, January 2003*, 38-44.

Arking, A. (1991), The radiative effects of clouds and their impact on climate, *Bull. Amer. Meteor. Soc*, *71*, 795-813.

Arking, A. (1999b), The influence of clouds and water vapor on atmospheric absorption, *Geophys. Res. Lett*, 26, 2729-2732.

Bender, F. A-M., H. Rodhe, R. J. Charlson, A. M. L. Ekman, and N. Loeb (2006), 22 views of the global albedo-comparison between 20 GCMs and two satellites, *Tellus, 58A*, 320-330.

Betts, A. K., and P. Viterbo (2005), Land-surface, boundary layer and cloud-field coupling over the south-western Amazon in ERA-40, *J Geophys Res*, *110*, D14108, doi: 10.1029/2004JD005702.

Betts, A. K. (2007), Coupling of water vapor convergence, clouds, precipitation, and land-surface processes, *J. Geophys. Res*, *112*, D10108, doi:10.1029/2006JD008191.

Betts, Alan K. (2009), Land□Surface□Atmosphere Coupling in Observations and Models, *J Adv Model Earth Syst*, *1*, art. #4, 18pp., doi: 10.3894/JAMES.2009.1.4.

Betts, A. K., M. Köhler, and Y. Zhang (2009), Comparison of river basin hydrometeorology in ERA-Interim and ERA-40 reanalyses with observations, *J. Geophys. Res*, *114*, D02101, doi:10.1029/2008JD010761.

Bony, S., and J. Dufresne, 2005, Marine boundary layer clouds at the heart of tropical cloud feedback uncertainties in climate models. *Geophys. Res. Lett.*, 32, 20.

Cess, R. and coauthors. (1997), Comparison of the seasonal change in cloud-radiative forcing from atmospheric general circulation models and satellite observations, J. Geophys. Res., 102(D14), 16593-16603.

Cess, R. D., M. Zhang, B. A. Wielicki, D. F. Young, X. Zhou, and Y. Nikitenko (2001), The influence of the 1998 El Niño upon cloud radiative forcing over the Pacific warm pool. *J. Climate*, 14, 2129–2137.

Charlock, T. P., and V. Ramanathan (1985), The albedo field and cloud radiative forcing produced by a general circulation model with internally generated cloud optics, *J. Atmos. Sci.*, 42, 1408-1429.

Coakley, J. A. JR., and D. G. Badwin (1984), Towards the objective analysis of clouds from satellite imagery data.

Del Geno, A. D., and A. B. Wolf (2000), The temperature dependence of the liquid water path of low clouds in the southern great Plains. J. Climate, 13, 3465-3486.

Dong, X., B. Xi, and P. Minnis (2006), A Climatology of Midlatitude Continental Clouds from the ARM SGP Central Facility. Part II: Cloud Fraction and Surface Radiative Forcing, *J. Clim*, *19*(9), 1765-1783.

Ellis, J. S., (1978), Cloudiness, the planetary radiation budget, and climate. Ph. D. thesis, Colorado State University, 129pp.

Harrison, E. F., P. Minnis, B. R. Barkstrom, V. Ramanathan, R. D. Cess, G. G. Gibson (1990), Seasonal variation of cloud radiative forcing derived from the Earth Radiation Budget Experiment, *J. Geophys. Res.*, 95, 18687-18703.

Kollias P., G. Tselioudis, B. A. Albrecht (2007), Cloud climatology at the Southern Great Plains and the layer structure, drizzle, and atmospheric modes of continental stratus, *J. Geophys. Res*., 112, D09116, doi:10.1029/2006JD007307.

Lazarus, S. M., S. K. Krueger and G. G. Mace (2000), A cloud climatology of the Southern Great Pains ARM CART. *J. Climate*, 13, 1762-1775.

Li, Z. and H. Leighton (1993), Global climatologies of solar radiation budget at the surface and in the atmosphere from 5 years of ERBE data. *J. Geoph. Res.* **98** D3 (1993), pp. 4919–4930.

Li, Z., and A. P. Trishchenko (2001), Quantifying uncertainties in determining SW cloud radiative forcing and cloud absorption due to variability in atmospheric conditions, *J. Atmos. Sci.*, 58, 376-389.

Mace, G. G., and S. Benson (2008), The Vertical Structure of Cloud Occurrence and Radiative Forcing at the SGP ARM Site as Revealed by 8 Years of Continuous Data, *J Clim*, *21*(11), 2591, doi:10.1175/2007JCLI1987.1.

Potter, G. L. and R. D. Cess (2004), Testing the impact of clouds on the radiation budgets of 19 atmospheric general circulation models, *J Geophys Res*, *109*, D02106, doi:10.1029/2003JD004018.

Ramanathan, V. (1987), The Role of Earth Radiation Budget Studies in Climate and General Circulation Research, *J. Geophys. Res.*, 92, 4075-4095.

Ramanathan, V., R. D. Cess, E. F. Harrison, P. Minnis, B. R. Barkstrom, E. Ahmad, and D. Hartmann (1989), Cloud radiative forcing and climate: Results from the Earth Radiation Budget Experiment, *Science*, 243, 57-63.

Rossow, W. B., and R. A. Schiffer (1991), ISCCP cloud data products, *Bull. Am. Meteorol. Soc.*, 72, 2-20.

Rossow, W., and Y.-C. Zhang (1995), Calculation of surface and top of atmosphere radiative fluxes from physical quantities based on ISCCP data sets 2. Validation and first results. J. Geophys. Res., D100, 1167-1197.

Schneider, S. H. (1972), Cloudiness as a global climatic feedback mechanism: The effects on the radiation balance and surface temperature of variations in cloudiness. *J. Atmos. Sci*., 29, 1413-1422.

Shi, L. (1994), Cloud radiative forcing on surface shortwave fluxes: a case study based on Cloud Lidar and Radar Exploratory Test. *J. Geophys. Res*., D99, 25909-25919.

Stokes, G. M., and S. E. Schwartz (1994), The Atmospheric Radiation Measurement (ARM) program: Programmatic background and design of the cloud and radiation test bed, *Bull. Am. Meteorol. Soc.*, 75, 1201-1221.

Vavrus, S. (2006), An alternative method to calculate cloud radiative forcing: Implications for quantifying cloud feedbacks, *Geophys Res Lett*, *33*, L01805.

Wielicki, B. A., E. F. Harrison, R. D. Cess, M. D. King, D. A. Randall (1995), Mission to Planet Earth: Role of Clouds and Radiation in Climate, *Bull. Amer. Meteorol. Soc.*, 76, 2125-2153.

Wielicki, B. A., T. Wong, N. Loeb, P. Minnis, K. Priestley, and R. Kandel (2005), Changes in Earth's Albedo Measured by Satellite, *Science*, 308, 825, doi: 10.1126/science.1106484.

Figure Caption

Figure 1. Diurnal (left), annual (middle) and interannual (right) variations of the normalized surface shortwave cloud radiative forcing (red solid), cloud fraction (green dashed) and cloud albedo (blue dashed dotted) from 1997-2009 ARM SGP measurements.

Figure 2. Scatter plots showing correlation between the normalized surface shortwave cloud radiative forcing and cloud fraction (a), cloud albedo (b), 2m air temperature (c), and 2m relative humidity RH (d). The colors of red, green and blue denote hourly, monthly, and annual averages, respectively.

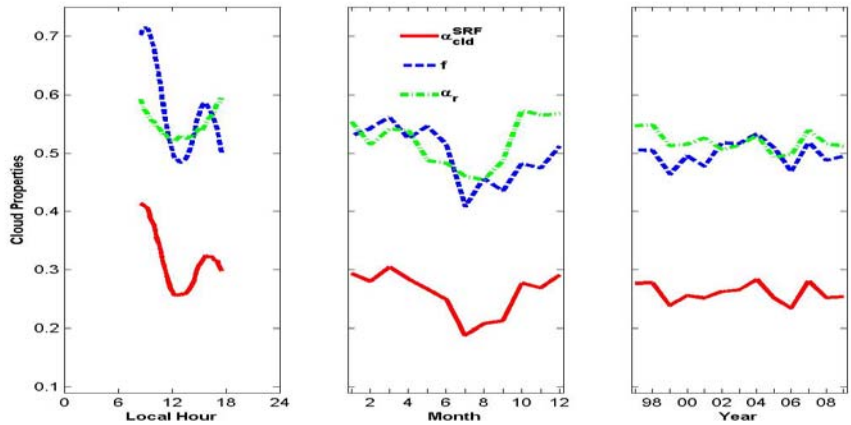

Figure 1

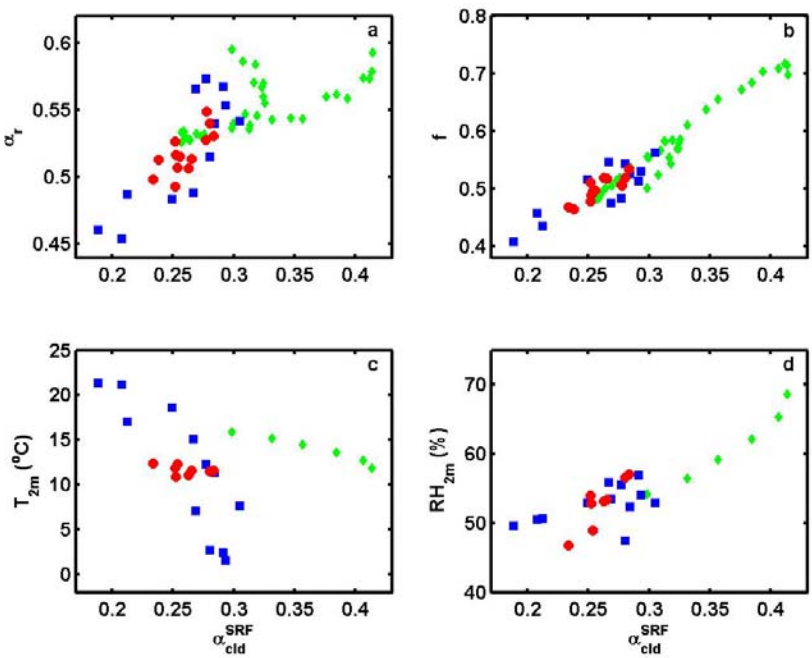

Figure 2